Supporting Information

Heterogeneous Fluorescence Intermittency in Single Layer Reduced Graphene Oxide

Jixin Si,[†] Sándor Volkán-Kacsó,[§] Ahmed Eltom,[‡] Yurii Morozov,[‡] Matthew P. McDonald,[‡]

Masaru Kuno,[‡] and Boldizsár Jankó[*,†]

[†]Department of Physics, University of Notre Dame, Notre Dame, Indiana 46556, United States
[‡]Department of Chemistry and Biochemistry, University of Notre Dame, Notre Dame, Indiana 46556, United States
[§]Noyes Laboratory of Chemical Physics, California Institute of Technology, 1200 East California Boulevard, Pasadena, California 91125, United States

[*] To whom correspondence should be addressed. Email: bjanko@nd.edu Fax: 574-631-5952

Supporting Information Discussions

Supporting Information Discussion 1: The mechanism of GO reduction

Under our experimental conditions, the temperature change of a single GO sheet caused by the absorption of light is estimated to be around 1K. Furthermore, the temperature change of the sp^2 domain in rGO is estimated to be ~4K. This suggests that the absolute temperature of GO/rGO during reduction lies below 500K, the typical temperature required to thermally desorb oxygen-containing functionalities. Thus a photo-thermal reduction mechanism is excluded. Instead, the initial bleaching of the emission is attributed to the migration of –OH groups, which gives rise to areas with a high concentration of functional groups. Subsequent multiple functional group chemistries then lead to the loss of water. The effective reduction then creates extended sp^2 networks, which in turn introduce fast non-radiative carrier relaxation pathways and corresponding blue-shifts in the emission spectrum. At the same time, direct dissociation of –OH also occurs together with the migration of C-O-C and possible dissociation of C-O-C/C=O/COOH groups. These latter processes continue to expand the size of initially produced sp^2 domains. However, they also lead to the loss of carbon atoms connecting these domains. Consequently, what results during later stages of GO reduction is a brightening and redshift of the emission spectrum since isolated sp^2 domains begin to take on single molecule behavior (Supporting Information Figure. S1).

Supporting Information Discussion 2: Explanation for the correlation between the evolution of the background intensity and the blinking power within the framework of the MRC model

The fluorescence intensity of the rGO sheet excited by continuous wave light undergoes an initial photo-brightening and a subsequent dimming phase (regions 2 and 3 in Ref. 22). This is evident in the evolution of the running median (~average) intensity (Supporting Information Figure. S2). The blinking power – approximated by the PSD integrated over the frequency range of estimation, 10^{-2} – 3 Hz – undergoes an almost identical time evolution (Supporting Information Figure. S3). According to Supporting Information Figure. S4 the blinking lags behind the intensity average by ~500s. We attributed the evolution of the intensity to the formation and subsequent destruction of fluorescent sp^2 clusters. Below, we explain the evolution of blinking and its correlation with the intensity.

Initially, fluorescent clusters emit steadily but within minutes some of them start blinking. These fluorescent clusters are found in significant numbers within the diffraction limited area projected unto any given pixel of the CCD. The total light intensity that falls on a pixel is the sum of the intensity contributions from all clusters: $I_{pixel}(\mathrm{t}) = \sum_m I_m(t) \int A(x - x_m, y - y_m)\, dxdy$. $I_m(t)$ is the intensity trajectory of cluster m, and the integration runs over the pixel area S_{pixel}. The convolution (summation) with the aperture function $A(x,y)$ ensures that the effective summation runs over fragments within the first Airy disk from the area imaged by the pixel.

Non-blinking clusters contribute only to the average (background) fluorescence. Blinking clusters will be described using the MRC model. For a single cluster, changes in non-radiative rates lead to fluctuation of fluorescence intensity,[i]

$$I_{\mathrm{single}}(t) = \frac{k_e\, k_r}{k_r + k_0 + \sum_{i=1}^{N} k_i\, \sigma_i(t)} \qquad \text{(S1)}$$

where k_e, k_r, k_0 are the excitation, radiative and background non-radiative rates respectively and k_i is the change of rate when an RC switches from a passive to an active state. The variable σ_i switches between 0 and 1 (passive/active states) with a frequency γ_i.

We propose that as the rGO specimen breaks up due to photolysis, RCs are created in the proximity of some clusters. This, in turn, initiates their blinking. We assume that typically not more than one RC is created at each cluster. Consequently, the cluster intensity fluctuation can be described as a telegraph process,

$$I_m(t) = I_{d,m} + (1 - \sigma_m(t))\big(I_{b,m} - I_{d,m}\big), \qquad \text{(S2)}$$

where $I_{b,m} = \frac{k_{e,m}\, k_{r,m}}{k_{0,m}+k_{r,m}}$ and $I_{d,m} = \frac{k_{e,m}\, k_{r,m}}{k_{0,m}+k_{r,m}+k_m}$. The rates are individual excitation (k_e), radiative relaxation (k_r), background (passive RC) non-radiative (k_0) and active RC non-radiative (k) rates.

In order to explain the correlation between the evolution of the running average and blinking power, we now look at statistical quantities averaged over time sections (Supporting Information Figures. S2-S4) along trajectories. We assume that clusters undergo negligible variation of emission and relaxation rates both in time and space across clusters. Then, the long-term behavior is due to the change in the number of blinking and non-blinking clusters. Empirically, we propose that blinking occurs within an average lag time of τ after a cluster has been created. The evolution of the number of blinking clusters can be cast as a function of the total number of clusters, $N_{pix,blink}(t) = r\, N_{pix}(t-\tau)$, where r is the fraction of blinking clusters. Thus, the running average is $\langle I_{pixel}\rangle_T(t) = I_b N_{pix}(t) - (I_b - I_d)\,\langle\sigma\rangle_T\, r\, N_{pix}(t-\tau)$, where the first term is dominant, since in regions 2 and 3 the blinking fluctuation is small compared to the average. Consequently, to a good approximation the running average of the intensity is $\langle I_{pixel}\rangle_T(t) \sim I_b N_{pix}(t)$. On the other hand, the total power of the blinking fluctuations is identical

to the variance integrated over time. Assuming that this identity holds for the sections in Supporting Information Figures. S2-S4, we find that $S_{pix,T}(t) = (I_b - I_d)^2 var_T\{\sigma\}\, r\, N_{pix}(t-\tau)$, which is due to the central limit theorem. This establishes the strong, time-shifted correlation between the running average and the power of fluctuation in Supporting Information Figure. S4.

Note, however, that there is no significant correlation between the simulated minimum number of switching channels and the background intensity or the PSD (see Supporting Information Figure. S5). This corroborates our assumption that the switching rate of RCs is stable during the photo-reduction process. Nevertheless, we cannot rule out the alternative explanation that the variation in the blinking power and slope follows from the relative time evolution of the various rates k_r, k_0 and k_i.

Supporting Information Discussion 3: The sectioning of trajectories

The emission trajectory for each CCD pixel is divided into small sections. These sections overlap with each other to obtain a smooth, temporally dynamic view of the blinking evolution. The brightening and dimming of the 'background' emission intensity is not reflected in the PSD spectrum when we exclude low frequency components.

The first five sections have lengths of 300 s each, while subsequent sections have lengths of 800 s. There are two reasons for choosing shorter lengths in the first five sections. First, there is little blinking in these stages and second as the section number increases, the blinking will emerge in the 'tail' part of the section. This significantly changes the PSD of that whole section. The first several sections are chosen to be short so that we can study the emergence of blinking with higher time resolution.

Supporting Information Discussion 4: Extracting the minimum number of switching channels of RCs from the PSD

We assume that in the resolution limited area of the CCD apparatus there may be several kinds of chemical species or structures acting as RCs. Each kind of RC has a specific structure/chemistry and thus a specific switching rate that shows up as a single Lorentzian component in the PSD. A group of identical RCs has a specific switching frequency between two different non-radiative rates. We call the collective contribution of these RCs a switching channel. We propose to extract the minimum number of switching channels by fitting the theoretically simulated PSD with its experimentally estimated counterpart, using available confidence intervals.

First, we calculate the theoretical PSD. It is a sum over Lorentzian components for all frequencies,

$$S_{xx}(\omega) \sim \sum_{i=1}^{N} \frac{\gamma_i}{\pi*(\omega^2+{\gamma_i}^2)} \qquad \text{(S3)}$$

where $S_{xx}(\omega)$ is theoretical PSD at frequency ω, γ_i is the rate at which an RC switches between a passive ($\sigma_i(t) = 0$) and active ($\sigma_i(t) = 1$) state, and N is the number of channels. In Supporting Information Eq. (S3) we assume that the number of RCs for each channel is the same. Furthermore, as we did in our earlier studies of blinking in a wide variety of fluorophores, we choose γ_i to have a power law distribution with exponent β. Also, we fix the highest and lowest frequency of the RCs to be 3Hz and 0.001Hz, respectively.

Next, in order to test whether a theoretical PSD fits within the confidence intervals of the experimental PSD, we calculate the quantity,

$$\epsilon = \sum_{j=1}^{N} \left(\frac{S_{experimental}(\omega_j) - S_{theoretical}(\omega_j)}{\delta_{experimental}} \right)^2 \qquad \text{(S4)}$$

for all possible combinations of γ_i and N. There are 23 ω_j and we choose $\epsilon = 20$ as the upper threshold of ϵ to decide whether to accept the combination. The minimum acceptable N is found for each pixel and plotted as a contour map in Supporting Information Figure. 2b.

Supporting Information Discussion 5: Spatial correlation in blinking (SC)

In order to estimate the experimental spatial correlation, we calculated the cross power spectral density (CPSD) of every pair of pixels in a 16x21 rectangular area of a single layer GO sheet. The same periodogram windows[i]were used as in the calculation of the PSD. CPSDs are normalized with respect to the PSDs of the pixel pair. Normalized CPSD values are then averaged over equidistant pixel pairs to yield the SC.

In Supporting Information Figure. S6 we also calculated the apparent correlation profile due to diffraction from the optical system, when the blinking is in fact spatially uncorrelated. We used a common Gaussian approximation for the aperture function. Parameter details can be found in the caption of Supporting Information Figure. S6.

Note that in Supporting Information Eq. (S3) we require that excitons recombine in the same cluster where they were initially created. Alternatively, we speculate that since the clusters are likely interconnected, the excitons might efficiently hop between neighbouring sites. The hopping may further result in spatially correlated blinking, which we plan to investigate.

Supporting Information Discussion 6: GO/rGO Properties

Supporting Information Figures S7-S11 contain important details of GO, rGO, and the GO-to-rGO photolytic conversion process. References ii and iii provide additional information as well as a comprehensive overview of the sample preparation and the photolysis mechanism.

Supporting Information Discussion 7: Confidence interval estimation for the power law

We performed ordinary least square (OLS) linear regression of log(frequency) versus log(PSD) to estimate the power law exponent. The estimation is the slope from linear fitting. The standard deviation (SD) of the power law exponent for all pixels in every section is smaller than 0.09, as shown below in Supporting Information Figure S12. SDs of exponents for most pixels are below 0.05.

Since the OLS assumes that the PSD estimates at different frequencies are statistically independent, we performed a correlation analysis. The PSD estimations were found to be either not correlated or positively correlated for the majority of frequency combinations. From a geometrical perspective, this implies a smaller probability of a line fit that crosses with the OLS fit. Large variations in the slope can only be achieved by a high probability associated with such crossing fit. In other words, positive correlations favor a smaller confidence interval for the slope. Therefore, by neglecting these positive correlations we are actually providing a more conservative estimation. Hence, the correlation analysis provides strong support in favor of the validity of the OLS error estimation.

Supporting Information Figures

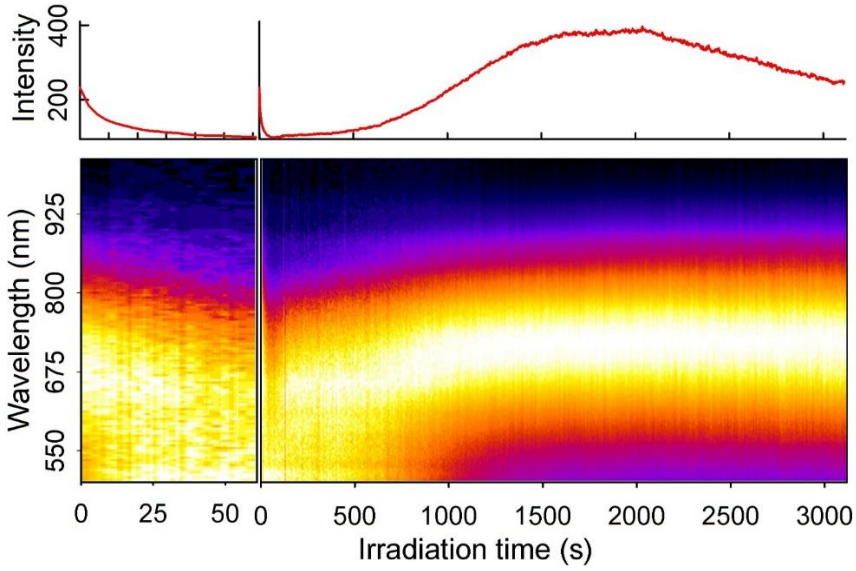

Supporting Information Figure S1. Waterfall plot of a single layer GO/rGO emission spectrum. This displays the evolution of the spectrum during reduction. The top panel is the emission intensity with respect to time. The left bottom panel gives a closer view of the rapid blueshift during the first 50s of bleaching. Afterwards, there is a significant gradual redshift accompanied by brightening and blinking until the photo-induced destruction of the rGO sheet.

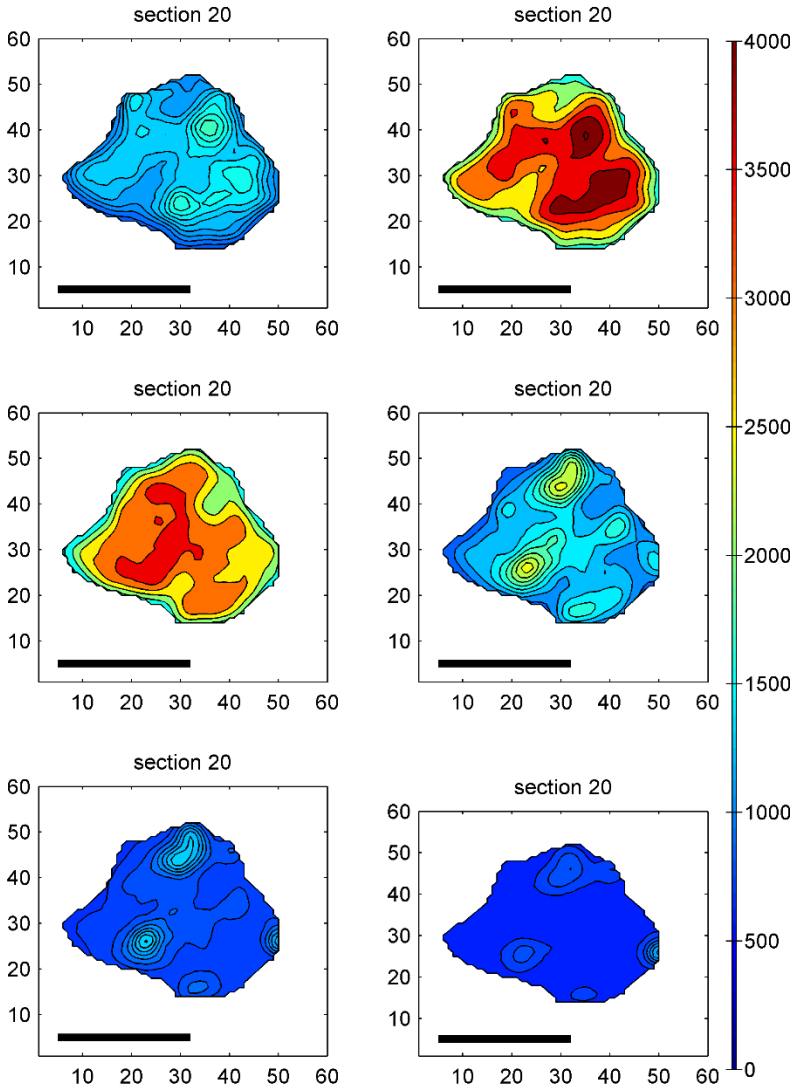

Supporting Information Figure S2. Temporal evolution of median intensity. The median is calculated over the temporal sections. Units of intensity: counts 10Hz. Scale bar: 5µm.

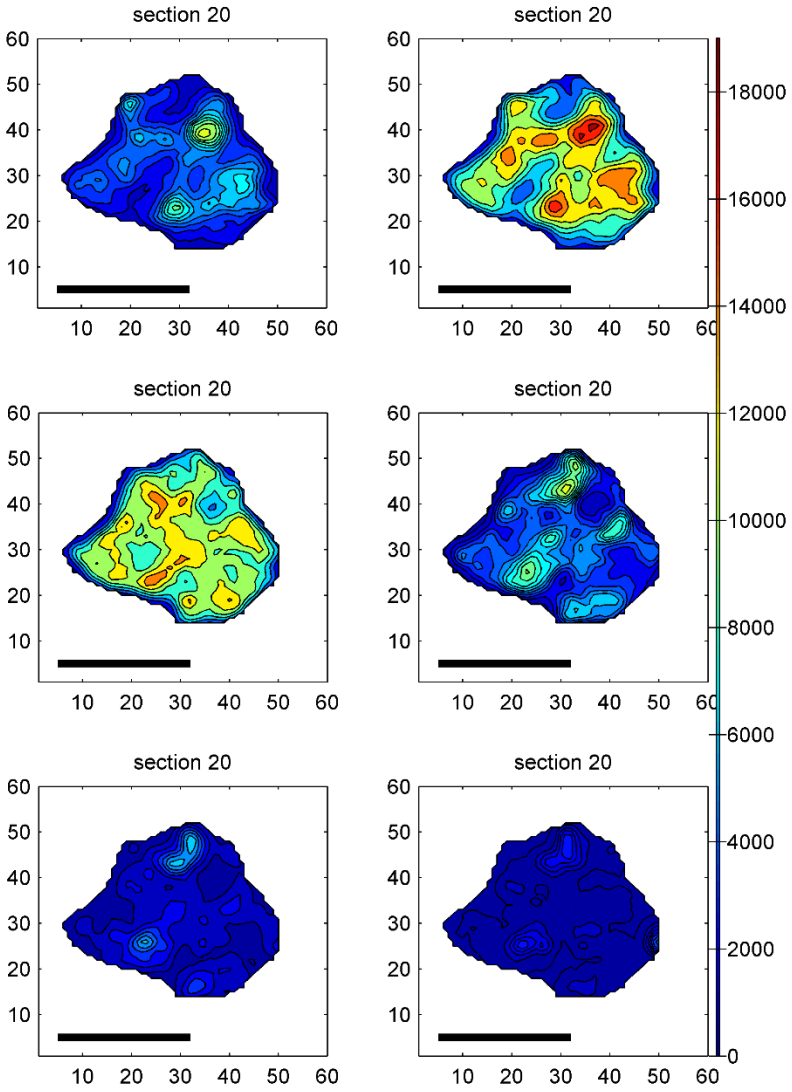

Supporting Information Figure S3. Temporal evolution of integrated PSD. The PSD of each temporal section is integrated over frequency. According to the Wiener-Khinchin theorem, this quantity equals the expectation value of the square of emission intensity. Units of integrated PSD: counts^2 (10Hz)^2. Scale bar: 5μm.

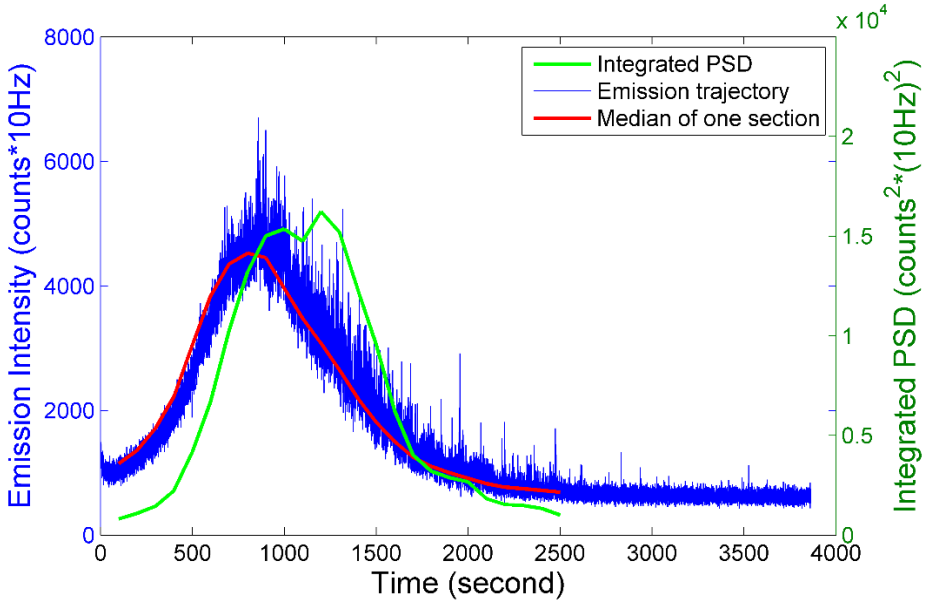

Supporting Information Figure S4. A comparison of emission intensity and integrated fluctuation PSD of one pixel (32, 32). The median of each section of a 100s length is plotted as a function of the initial time of that section, hence it is shifted to the left. For consistency, the time evolution of integrated PSD is plotted in the same way.

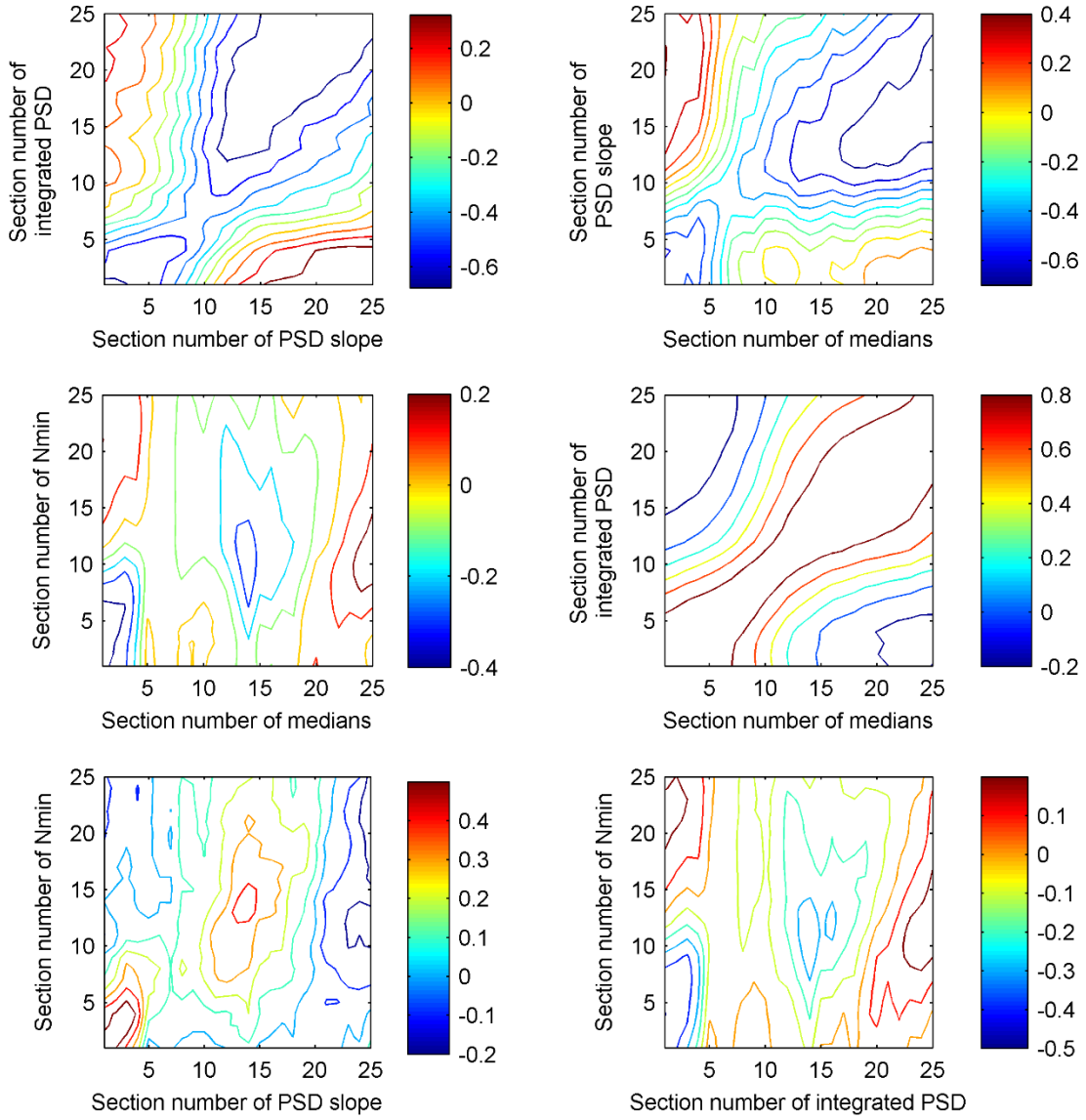

Supporting Information Figure S5. Pair correlation of intermittency parameters. Contour plots of correlation between blinking power (integrated PSD), PSD slope, fluorescence intensity median, and minimum number of switching channels of RC. There is a clear correlation between intensity median and integrated PSD, with a shift of 5 sections (cf. the plot shown right column, second row). There is positive correlation between integrated PSD and the slope of PSD when the

sections are close. Thus the shifted positive correlation between intensity median and integrated PSD is expected and observed. There is hardly any correlation between these variables to minimum number of switching channels of RC.

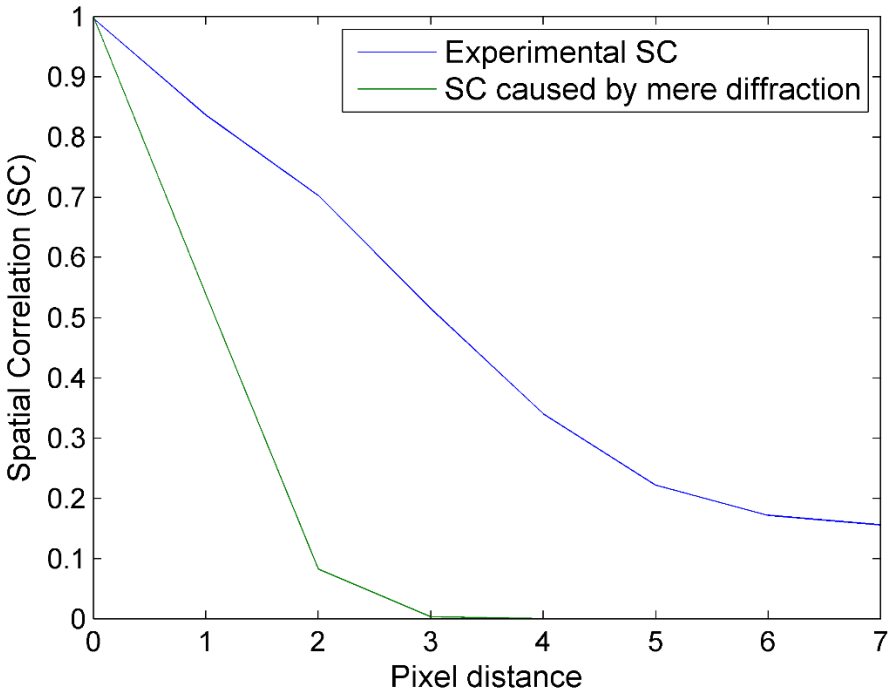

Supporting Information Figure S6. Comparison of experimental spatial correlation (blue line) and theoretical spatial correlation (green line) generated merely by diffraction. The optical system uses an objective with a numeric aperture of 1.4 and with a 100x magnification. The radius of Airy disk of a 600nm light is 26.1 micrometers. We approximated the Airy pattern with a Gaussian function and calculated the cross power spectral density (CPSD) as a representation of spatial correlation. The length of one pixel distance is 178 nm.

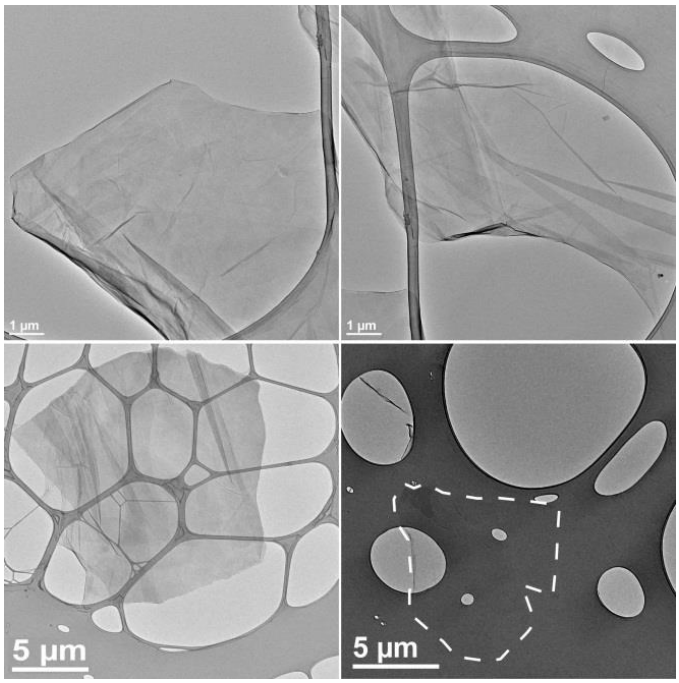

Supporting Information Figure S7. Transmission electron microscopy (TEM) micrographs of individual GO sheets.

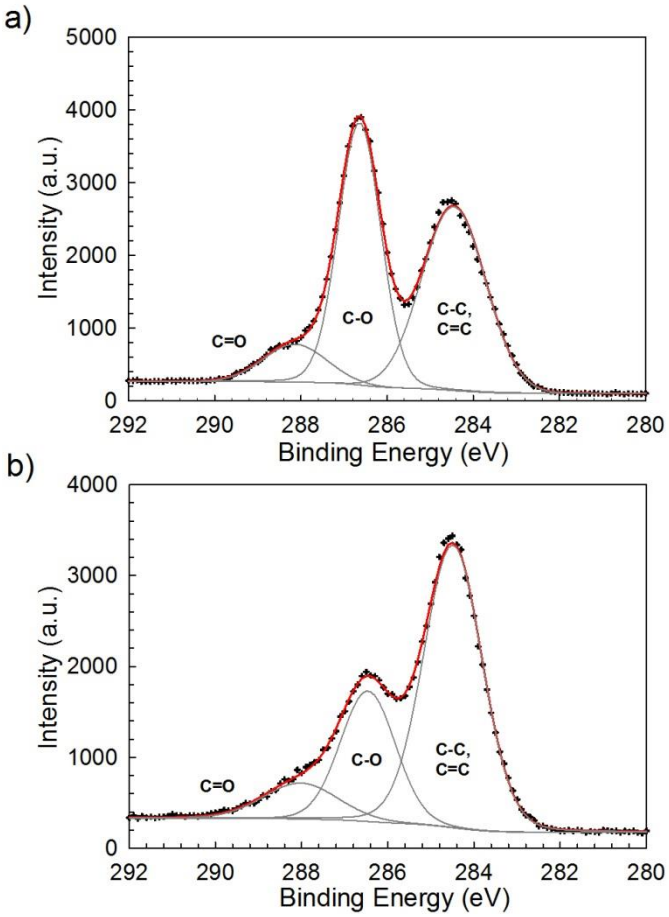

Supporting Information Figure S8. Ensemble X-ray photoelectron spectroscopy (XPS) measurements of GO's C1s peak before (a) and after (b) 990 minutes of 405 nm laser irradiation (I_{exc}~0.2 Wcm^{-2}).

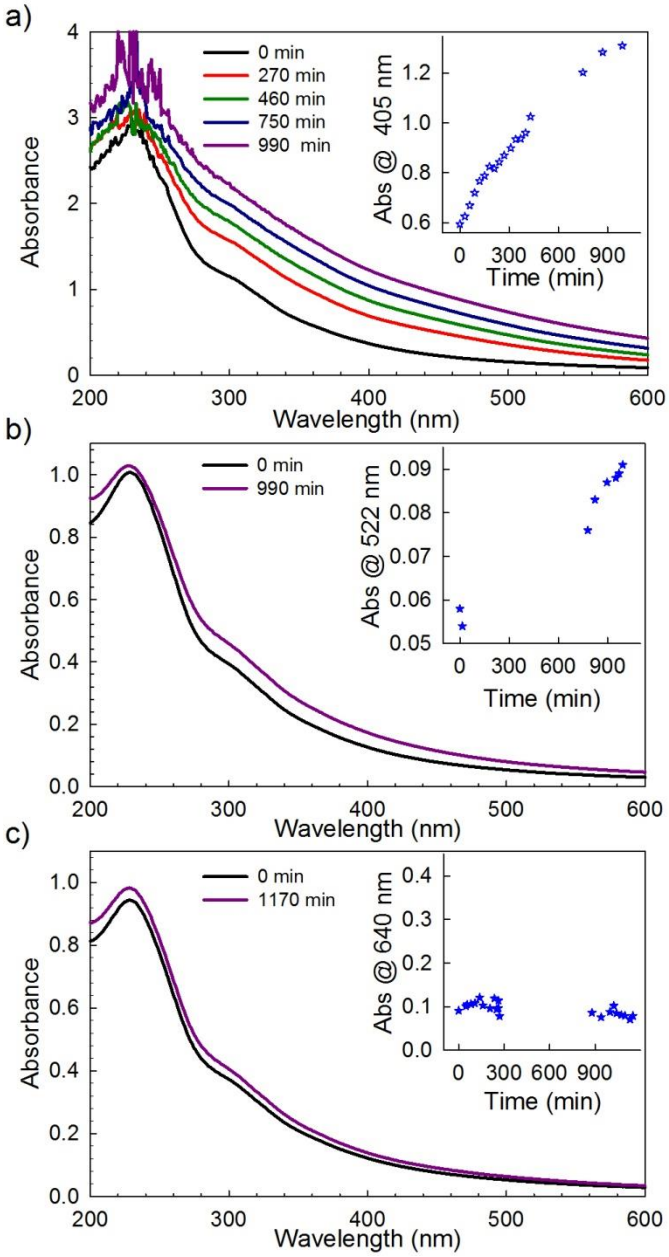

Supporting Information Figure S9. UV-Visible absorbance spectra of a GO ensemble as a function of irradiation time for (a) 405 nm [I_{exc}~0.2 Wcm^{-2}] (b) 522 nm [I_{exc}~0.13 Wcm^{-2}], and (c) 640 nm [I_{exc}~0.21 Wcm^{-2}] excitation. The insets show the time evolution of their absorption at a given wavelength.

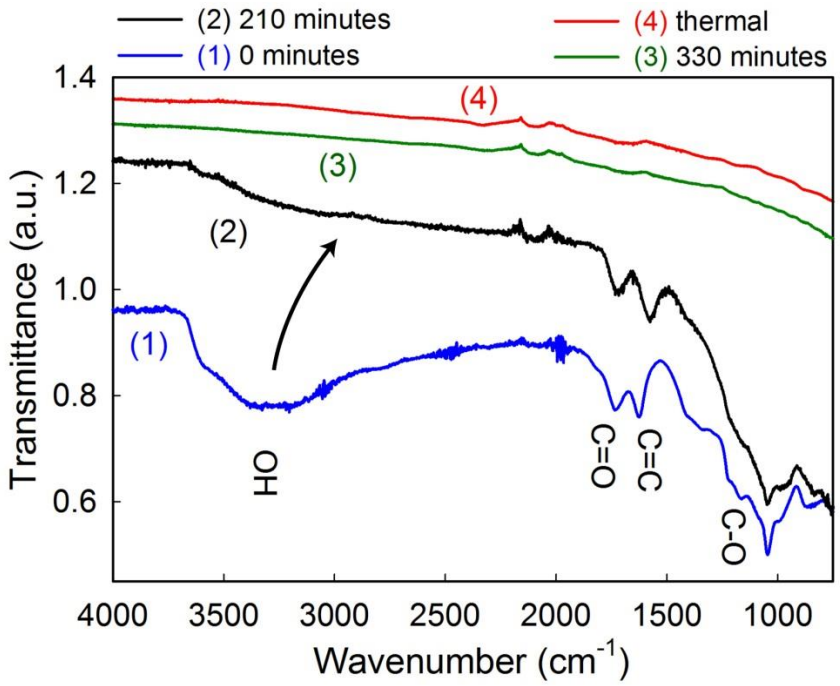

Supporting Information Figure S10. FTIR transmittance spectra of GO thin films subjected to 0 minutes (1; blue line), 210 minutes (2; black line), and 330 minutes (3; green line) of laser irradiation (λ_{exc} = 405 nm; I_{exc} = 2 Wcm^{-2}). Trace (4) shows the FTIR spectrum of a thermally reduced (following the procedure of ref. [iv]) GO thin film. Between traces (1) and (2), the most striking feature is the dramatic decrease in OH absorbance (2500 – 3700 cm^{-1}). The epoxide peaks (1225 and 1137 cm^{-1}) and carbonyl/carboxyl peak (1712 cm^{-1}) also decrease, although not as dramatically as OH. After 330 minutes (3), all peaks associated with oxygen functionalities disappear and the spectrum closely resembles thermally reduced GO (4) as well as literature rGO spectra.[v] Spectra are averaged over 40 scans on a Shimadzu IRPrestige21 spectrometer implementing a PIKE MIRacle single reflection ATR (N_2 purged) with a spectral resolution of 2 cm^{-1}.

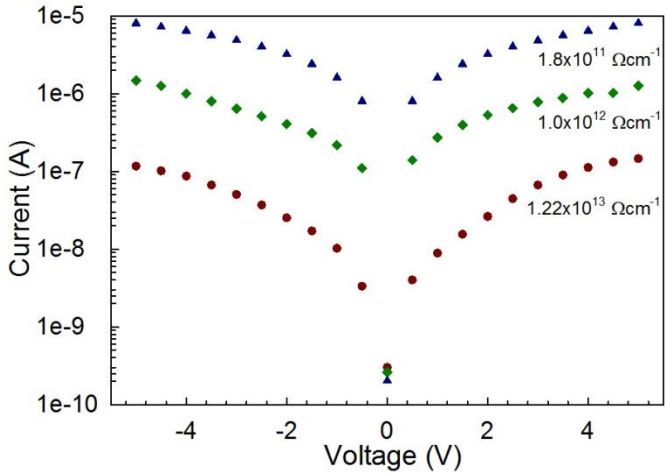

Supporting Information Figure S11. Ensemble two-probe transport measurements of GO (red circles), rGO (from a GO thin film, 75 minute irradiation time, green diamonds), and rGO (from a GO suspension, 990 minutes irradiation time, blue triangles). In either case, GO was reduced with λ_{exc}= 405 nm and I_{exc} ~0.2 Wcm^{-2}. Electrode gaps are ~60 µm.

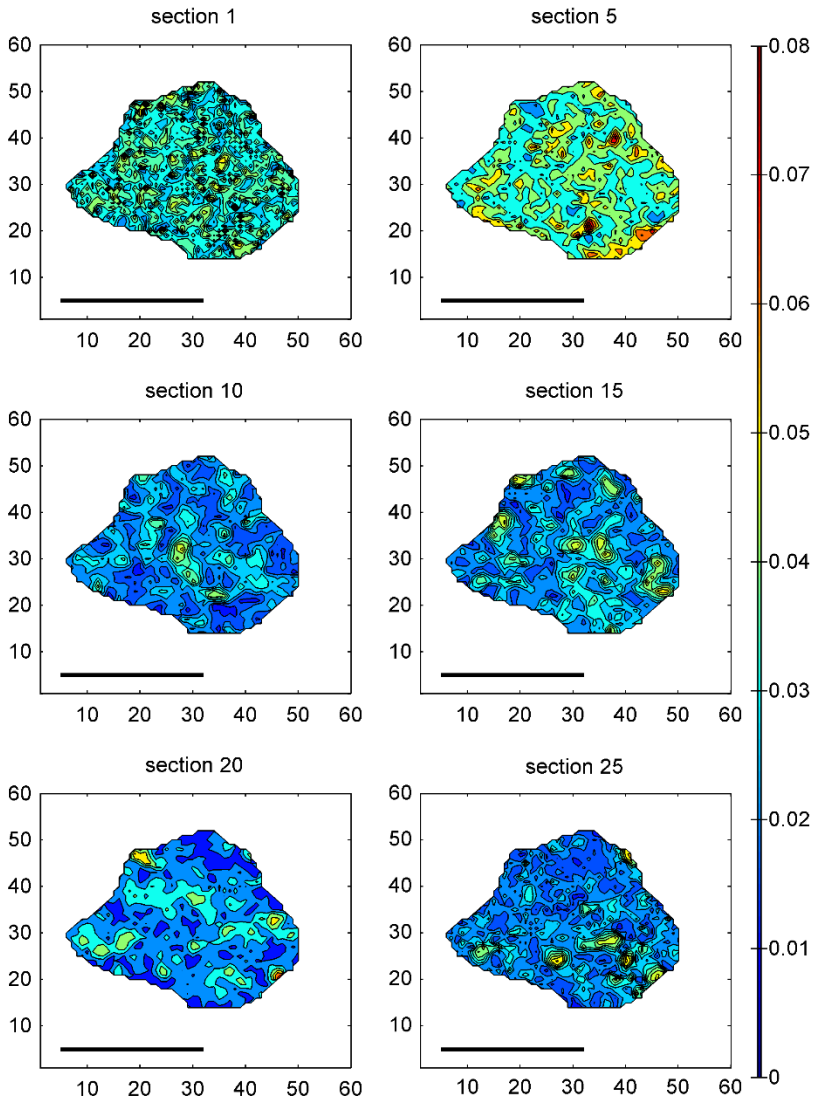

Supporting Information Figure S12. Contour plots for the standard deviation of power law exponent at different sections. Scale bar: 5 μm.

[i] Frantsuzov, P. A.; Volkán-Kacsó, S and Jankó, B. *Nano Lett.* **13** (2), 402-408 (2013)

[ii] McDonald, M. P.; Eltom, A.; Vietmyer, F.; Thapa, J.; Morozov, Y. V.; Sokolov, D. A.; Hodak, J. H.; Vinodgopal, K.; Kamat, P. V.; Kuno, M. Direct Observation of Spatially Heterogeneous Single-Layer Graphene Oxide Reduction Kinetics. *Nano Lett.* **2013,** *13,* 5777–5784.

[iii] Sokolov, D. A.; Morozov, Y. V.; McDonald, M. P.; Vietmeyer, F.; Hodak, J. H.; Kuno, M. Direct Observation of Single Layer Graphene Oxide Reduction through Spatially Resolved, Single Sheet Absorption/Emission Microscopy. *Nano Lett.* **2014,** *14,* 3172–3179.

[iv] Wang, Z.-L., et al. *Chem. Commun.* **2012**, *48*, 976-978.

[v] Chen, W.; Yan, L. *Nanoscale* **2010**, *2*, 559-563.